Flow over a Trailing Flap and Its Asymmetric Wake

S. Acharya,* D. Adair,† and J. H. Whitelaw‡
Imperial College, London, England

Detailed measurements of pressure and velocity characteristics are reported for the attached flow on a trailing flap and in its downstream asymmetric wake. The results indicate that the flow over the flap is subjected to an adverse pressure gradient. Near the trailing edge, an inflection point develops in the streamwise velocity profile and the flow approaches intermittent separation. The wake is asymmetric with a destabilizing curvature on the suction side and a stabilizing curvature on the pressure side. Streamwise variations in the near wake are primarily confined to the inner layer, and further downstream the mean velocity and turbulence quantities attain self-similar profiles. Nonequilibrium effects are present in the near wake and imply that mixing length models are not appropriate. Both the pressure gradient term and the cross-stream gradient of the turbulent stresses are found to be important. Streamwise gradients of the turbulent stresses are, however, small.

Nomenclature

b = width of the upper part ($y/\delta > 0$) of the wake
B = constant in the law of the wall equation
c = chord length (Fig. 1)
c_p = pressure coefficient
c_{pw} = pressure coefficient along the flap surface
$c_{p\infty}$ = freestream pressure coefficient
k = constant in the law of the wall equation
l_p = distance from the wake center to the point where the streamwise velocity defect in the pressure side is half the maximum defect
l_s = distance from the wake center to the point where the streamwise velocity defect in the suction side is half the maximum defect
L = mixing length
n = normal distance from the flap surface
p = pressure
q = kinetic energy of turbulence
s = distance along the surface measured from the trip wire
$\bar{u}, u'$ = mean and fluctuating velocity in the streamwise direction
$\overline{u'v'}$ = mean shear stress
$\overline{u'^2}$ = mean normal stress in the streamwise direction
$\bar{u}_c$ = mean streamwise velocity at wake center
$\bar{u}_{eu}$ = mean streamwise velocity in the suction-side freestream
$\bar{u}_{el}$ = mean streamwise velocity in the pressure-side freestream
$\bar{u}_{\text{ref}}$ = mean reference velocity in the streamwise direction
$\bar{v}, v'$ = mean and fluctuating cross-stream velocity
$\overline{v'^2}$ = mean normal stress in the cross-stream direction
$\overline{w'^2}$ = mean normal stress in the spanwise direction
x, y = streamwise coordinate in the wake measured from the trailing edge, and cross-stream coordinate
δ = boundary-layer thickness, i.e., the distance from the wall where the velocity reaches 99.5% of the freestream velocity
δ_1 = displacement thickness, $\int_0^\delta \left(1 - \frac{\bar{u}}{\bar{u}_{eu}}\right) dy$
δ_2 = momentum thickness, $\int_0^\delta \frac{\bar{u}}{\bar{u}_{eu}}\left(1 - \frac{\bar{u}}{\bar{u}_{eu}}\right) dy$
ν = kinematic viscosity
ϕ = angle of the flow vector
ρ = density in the isothermal flow

Received Dec. 9, 1985; revision submitted July 28, 1986. Copyright © American Institute of Aeronautics and Astronautics, Inc., 1987. All rights reserved.

*Assistant Professor, Department of Mechanical Engineering, Louisiana State University, Baton Rouge, LA.
†Research Assistant, Department of Mechanical Engineering, Imperial College, London, England.
‡Professor, Fluids Sections, Department of Mechanical Engineering, Imperial College, London, England.

Introduction

THE flow in the vicinity of the trailing edge of a high-lift aerofoil is subjected to strong adverse pressure gradients and involves strong interaction between the inviscid flow and nonequilibrium turbulent boundary layers, streamline curvature, and an asymmetric wake. The current ability to predict such flows is unsatisfactory[1] due, in part, to the limited understanding of the flow in the neighborhood of the trailing edge. The present work describes one of a series of experiments designed to improve the understanding of the structure of turbulent flow over high-lift aerofoils as a function of the angle of attack. In the earlier experiments,[2,3] trailing flaps with a deflection angle of 17.5 and 16 deg led to regions of separated upper-surface flow. The present work provides detailed measurements of pressure, mean velocity, and turbulence quantities for the attached flow over a flap at a deflection angle of 14 deg and in its asymmetric downstream wake.

A number of studies have been reported on the flow around the trailing edge of a flat plate[4-9] and a symmetric aerofoil,[10-14] and recently Nakayama[15] and Viswanath et al.[16] have investigated the flow in the trailing edge region of an asymmetric aerofoil. In Ref. 15, the flow near the trailing edge at 0 and 4 deg incidence was observed to be attached while a separation bubble appeared at the trailing edge at an angle of attack of 12 deg comparable to that of the present arrangement. In Ref. 16, measurements were obtained for subsonic attached flow (freestream Mach number = 0.4) on a trailing flap at a deflection angle of 12.5 deg. In this paper, the flow characteristics for an attached trailing-edge flow at an angle of deflection of 14 deg with a freestream Mach number of 0.072 are examined.

Flow Configuration and Instrumentation

The experiment was conducted in the 450 × 310-mm working section of the low-speed wind tunnel described by Crabb.[17] The model configuration (see Fig. 1), spanned the working section and comprised a 1035-mm flat plate placed at an incidence angle of 1 deg to the floor of the tunnel, a 249-mm trailing plate set at 13 deg deflection and connected to the flat

plate by an arc of radius 749.25 mm. Potential flow existed over a region of around 230 mm above the trailing edge and also in a 82 mm region underneath. The reference parameters associated with this arrangement are given in Table 1.

Surface oil-flow visualization and spanwise pressure and hot-wire measurements were made to determine the extent of the two-dimensional flow. The visualization indicated that the flow was two-dimensional except within the immediate vicinity of the sidewalls, and this was also confirmed by wall pressure and hot-wire measurements which were identical within experimental errors in the central 320 mm of the flap. Spanwise profiles of velocity and pressure measured in the wake just downstream of x/c of 0.1 agreed to within 2% in the central 280 mm.

In regions of potential flow and for the calibration of hot-wires, a pitot-static probe with 2.2-mm o.d. was used. In other regions, a five-hole probe (calibrated as recommended in Ref. 18) was used to measure the flow angle and the static and dynamic pressure. The pitot-static probe gave mean velocity data within 0.7% and static pressure data within 1.0% of $\frac{1}{2}\rho\bar{u}^2$. In the boundary layer, the accuracy of the five-hole probe was within 1.5% of the local velocity, 4% of $\frac{1}{2}\rho\bar{u}^2$ for static pressure and 2 deg for the flow angle.

Hot-wire instrumentation and equations were used to interpret and calibrate the signal of stationary hot-wires (DISA 55P10 and DISA 55P61). The anemometers (DISA 55M10) were operated in the constant temperature mode with an overheat ratio of 1.8 and a cutoff frequency in excess of 100KHz. A DEC PDP8E computer was used to record and process the anemometer voltages. The mean velocity data obtained from the hot-wires were accurate to 2%, with the greatest uncertainty near the surface. The accuracy of the turbulence quantities varied with turbulence intensity so that, for example, the normal stresses are accurate to about 15% and shear stresses to about 11% at 15% turbulence intensity. Further details of the accuracy of the pressure and hot-wire probes used are given by Thompson.[19]

As will be seen later, the near-wall flow close to the trailing edge has very low velocities leading to the possibility of intermittent separation, in which case stationary hot-wire results are unreliable. For this reason, a number of measurements close to the trailing edge and in the near wake were made with the flying hot-wire arrangement described in Refs. 2 and 3, which is suitable for measurements in both forward and reversed flows. Results from the flying hot-wire were found to be close to those of the stationary hot-wire (within experimental uncertainty), indicating that although the flow is close to intermittent separation, instantaneous flow reversal does not actually occur.

Results and Discussion

Figure 2 shows lines of constant static pressure coefficient and mean velocity vectors which together provide an overview of the flow. The asymmetric nature of the wake is clear from the wake velocity vectors on either side of the trailing edge. The lines of constant c_p indicate that the boundary-layer flow experiences an adverse streamwise pressure gradient, while in the near wake, the flow behind the trailing edge is subjected to a favorable pressure gradient. The elliptical shape of the constant pressure coefficient lines in the vicinity of the trailing edge implies that the cross-stream pressure gradients are larger than those in the streamwise direction. The pressure distributions indicate that the largest streamwise and cross-stream gradients occur in the near wake region, and comparison with the results of Ref. 3 shows that the cross-stream gradients increase by an order of magnitude as the incidence angle is increased from 14 to 16 deg.

Table 1 Reference parameters

Parameter	Symbol	Value
Velocity	u_{ref}	25.00 m/s
Static pressure (relative to atmosphere)	P_{ref}	-156.38 N/m^2
Viscosity	ν	15.22×10^{-6}m^2/s
Density	ρ	1.197 kg/m^3
Temperature	T	20°C
Chord length	c	1.4394 m
Reynolds number	$Re=\frac{u_{ref}c}{\nu}$	2.36×10^6

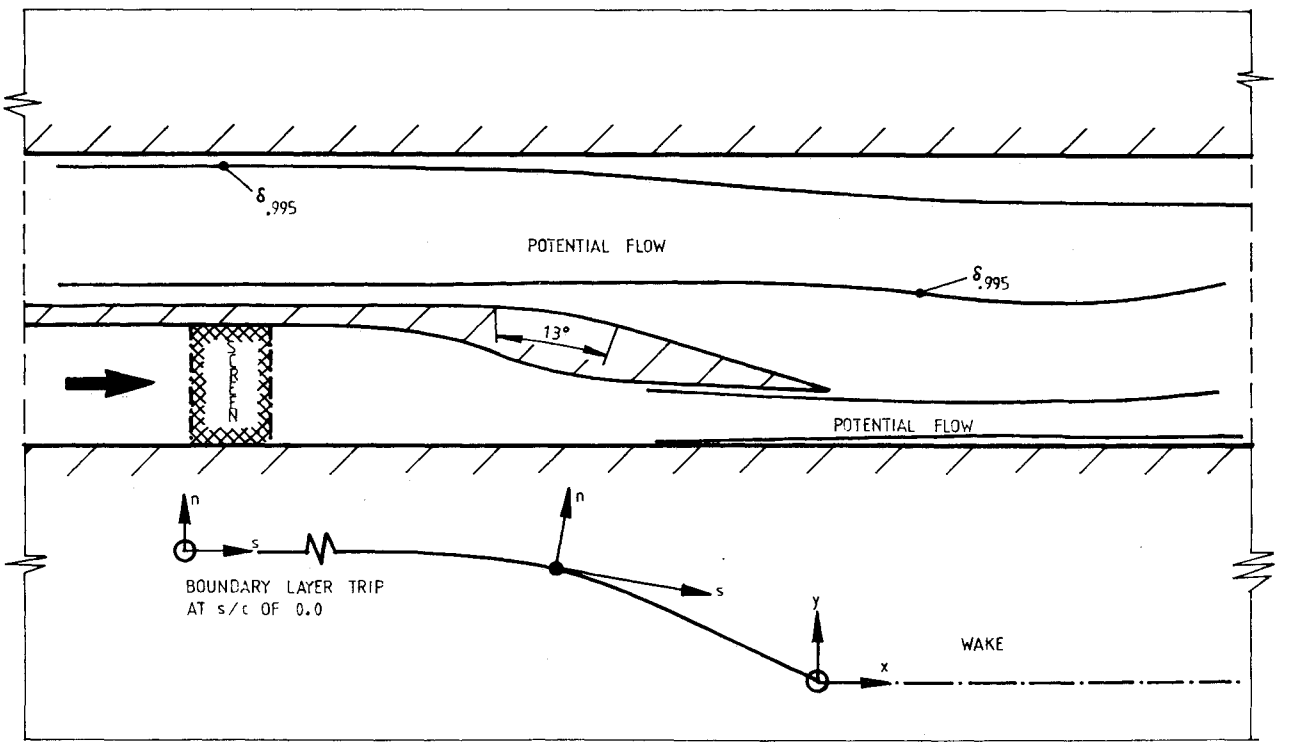

Fig. 1 Flow configuration.

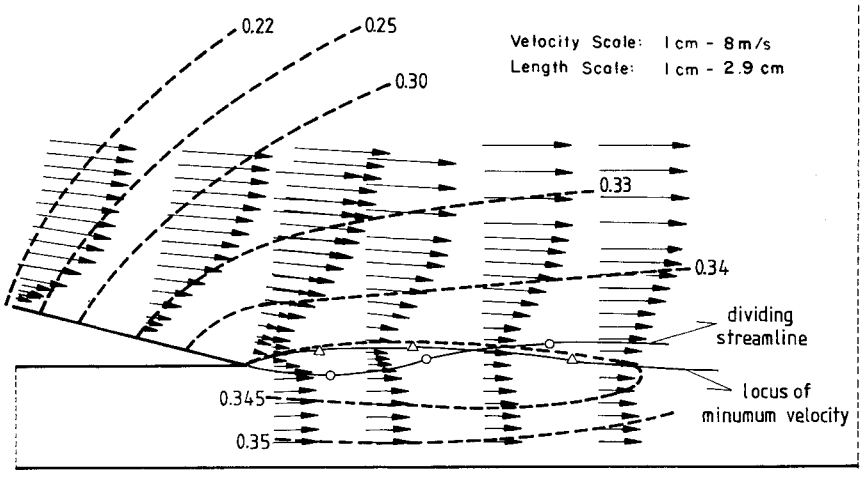

Fig. 2 Mean velocity vectors and contours of static pressure coefficient.

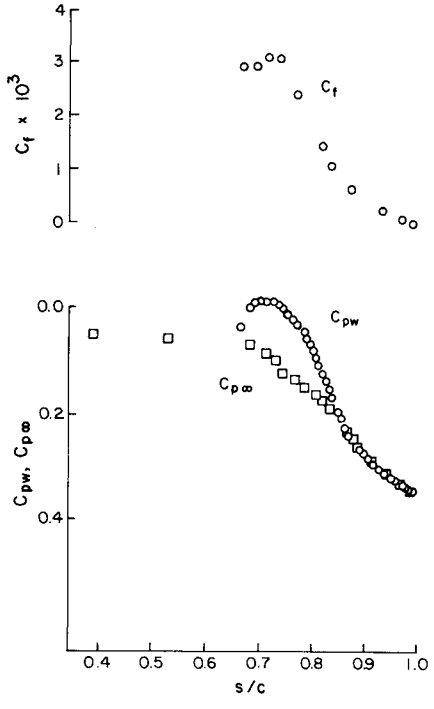

Fig. 3 Distribution of pressure coefficient ($c_{p\infty}$, c_{pw}) and skin friction coefficient c_f.

The surface curvature influences the suction-side static pressure coefficient from approximately 2.4% of chord upstream of the start of the curved surface, $s/c = 0.694$ (see Fig. 3), and in common with the results of Ref. 2, 3, and 16, initially decreases along the curvature and then recovers quickly to a much larger value. The freestream pressure coefficient, however, increases monotonically from the start of the curvature. Along the curved surface ($s/c = 0.694 - 0.85$), the two pressure coefficients have different magnitudes, with this difference decreasing towards the trailing edge. The skin friction coefficient c_f (Fig. 3) was obtained from Clauser charts and increases slightly due to surface curvature before decreasing with the adverse pressure gradient.

The freestream velocities (Fig. 4) develop in a manner consistent with the static pressure, and it should be noted that the suction-side freestream velocity in the wake is nearly twice that on the pressure side. This difference in the two freestream velocities is due to the mildly curved splitter plate in the wind tunnel contraction (upstream of the 1035-mm flat leading edge) and the screen on the pressure side (shown in Fig. 1), which is used as a flow straightener and to reduce spatial variations in turbulence quantities. As the flow is retarded by the pressure gradient, the boundary layer along the surface grows rapidly and the displacement and momentum thicknesses δ_1 and δ_2 rise rapidly to the trailing edge, where the shape factor δ_1/δ_2 and the ratio δ_1/δ have values of 2.2 and 0.2 respectively. These values imply (using Sandborn and Kline's[20] criteria) that the flow is close to intermittent separation, and this is reinforced by the small, though positive, values of c_f (Fig. 3) and the near-wall values of the streamwise velocity (Fig. 5) close to the trailing edge. However, as noted earlier, comparison of flying and stationary hot-wire results indicate that instantaneous flow reversal does not actually occur. In the wake, δ_1 and δ_2 decrease and the shape factor approaches unity.

Mean Velocity

The development of the upper-surface boundary layer is shown in Fig. 5. From Clauser chart plots of the velocity (not shown), the law of the wall, with $k = 0.41$ and $B = 5.0$, is found to be valid along the entire aerofoil surface, despite the deceleration of the streamwise flow to a near-separation condition as evident in Fig. 5a. The cross-stream velocity, also shown in Fig. 5a, increases by nearly an order of magnitude along the curved surface and is always less than 10% of the streamwise component. At $s/c = 0.98$, the streamwise velocity profile develops an inflection point in the central region of the boundary layer, and this propagates downstream into the wake. At higher incidence angles, the origin of the inflection point moves upstream, and the flow separates at $s/c = 0.93$ for 16 deg incidence[3] and $s/c = 0.87$ for 17.5 deg incidence.[2]

The velocity profiles of Fig 5b reveal the wake asymmetry that stems from the differing wall boundary layers on the pressure and suction sides. On the pressure side, the boundary layer is thin and the cross-stream gradients are confined to a narrow region near the trailing edge and are greater than the cross-stream gradients on the suction side. As on the suction side, the pressure-side velocity profile has an inflection point.

The location of the minimum streamwise velocity in the wake moves upwards from the trailing edge to $x/c = 0.0347$, beyond which it moves towards the pressure side; at $x/c = 0.347$, the flow has recovered to that of a plane mixing layer, which is characterized by the minimum wake velocity occurring in the pressure-side potential stream and the absence of the inflection point in the pressure-side velocity profile. With separated flow,[2,3] the wake was more pronounced and the location of minimum wake velocity moved rapidly upwards up to x/c of 0.344 for 16 deg incidence and up to x/c of 0.428 for 17.5 deg. Thus, the location of the minimum wake velocity where the shear stress changes sign, and the location of the inflection points where the intensities and the shear stress peak, are different in the wake of separated flows and are directly responsible for altering the distributions of the turbulence quantities.

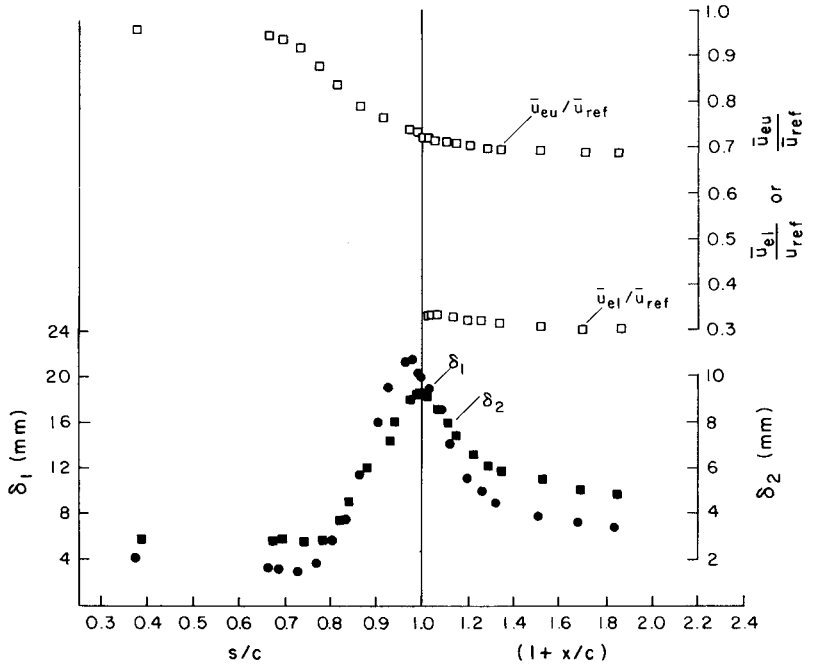

Fig. 4 Parameters of mean flow development (δ_1, δ_2, $\bar{u}_{eu}/u_{ref}$, $\bar{u}_{el}/u_{ref}$).

The pressure-side cross-stream velocity in the near wake increases up to x/c of 0.0139, followed by a decay indicating an initial rise in the wake curvature which is also seen in the dividing streamline in Fig. 2. At x/c of 0.208, the cross-stream velocity is nearly zero and the wake tends to a plane mixing layer. The corresponding locations for 16 and 17.5 deg incidence are 0.275 and 0.33 respectively, indicating the effect of increasing trailing-edge separation on wake development.

Examination of the near-wake profiles show that the upper part ($y/\delta > 0$) of the wake changes over its entire width with the larger variations in the inner regions, whereas the changes in the lower part ($y/\delta < 0$) are confined to the inner region, except in the very near wake ($x/\delta_2 = 1-2$). The asymmetric wakes of Refs. 15 and 16 and the separated wakes of Refs. 2 and 3 exhibit similar behavior, while the symmetric wakes of Refs. 5 and 15 indicate that the major changes occur only in the inner region.

The similarity of the near-wake profiles was examined by using the difference between the maximum and minimum velocities ($\bar{u}_{eu} - \bar{u}_c$) as the velocity scale, and the distances from the wake center to the points where the streamwise velocity defect is one-half the maximum velocity defect on the pressure and suction sides (denoted by l_p and l_s). The scaled velocities are plotted in Fig. 6 and indicate that similarity exists except near the outer edges of the very near wake. The present data in scaled coordinates compares well with those of Hah and Lakshminarayana,[14] and the similarity profile seems to follow the Gauss function $\exp[-0.6993(y/l_s)^2]$.

Reynolds Stresses

The distribution of Reynolds stresses along the suction surface are shown in Fig. 7 with the corresponding wake values in Fig. 8. Over the curved surface, the maximum normal stresses $\bar{u}'^2$ and $\bar{v}'^2$ decrease, due to curvature, by approximately 10% and 20% respectively, while $\bar{w}'^2$ remains almost unchanged. The maximum shear stress decreases by about 27% along the curvature with large decreases in the outer region.

Downstream of the curvature, the maximum stresses increase by around 30% at the trailing edge due to the adverse pressure gradient that also causes the (y/δ) location of the peak Reynolds stresses to increase to a value of around 0.3. Beyond s/c of 0.928, the near-wall velocity gradient diminishes (Fig. 5a) and the Reynolds stress production and the Reynolds stresses themselves decrease; thus, at $s/c = 0.98$, the near-wall stresses are nearly the same as at $s/c = 0.946$. Further downstream, the decrease of $\partial\bar{u}/\partial n$ near the wall is reduced, and the normal stresses show a gradual increase primarily due to diffusion from the central region of the boundary layer. The region $0.928 < s/c < 0.946$ is associated with the inflection point in the streamwise velocity profile moving upwards from the surface. For separated flows,[2,3] the inflection point is similarly deflected upwards and around the trailing-edge separation bubble and, as in the present flow, turbulent diffusion from the inflection point to the near-wall region plays an important role.

In the very near wake, rapid changes occur around the wake centerline, while the corresponding changes in the outer regions are relatively gradual. The normal stress profiles in the near wake exhibit two maxima; the first occurs near $y/\delta = 0$ and corresponds to the inflection point in the pressure-side velocity profile, and the other is located at a value of y/δ in the range of 0.15-0.35, where the inflection point in the suction-side velocity profile occurs. With streamwise development, the mixing process smooths out the smaller peak near the centerline and the normal stresses decrease outward from a single peak at $y/\delta < 0.3$. This decay in the smaller peak intensity is slowest for the streamwise component as is also observed in the asymmetric wake data of Refs. 14 and 15. As in Ref. 15, the turbulent stresses in the upper part of the wake increase (with the suction-side maxima increasing by 10–20%) up to $x/c = 0.0347$ due to adverse pressure gradient and destabilizing streamline curvature; beyond x/c of 0.0347, the stresses gradually decay. On the pressure side, the turbulent intensities show only small variations in the streamwise direction due to the counteracting effects of turbulent diffusion and stabilizing streamline curvature. At higher incidence angles, the wake is more pronounced and the wake center shifts upwards.[2,3] Due to the higher production-to-dissipation ratio in the near wake of such flows, the turbulent stresses are higher at the larger incidence angles, and since the wake center has moved upwards, the turbulent stresses peak at a larger y/δ value. The flows in Refs. 2 and 3 also recover to a plane mixing layer but at much greater distances from the trailing edge; for example, the double-peak intensity profiles of the present flow reduces to a single-peak profile at $x/c = 0.07$, while for 16 and 17.5 deg incidence, the corresponding values are approximately 0.275 and 0.35 respectively. Consistent with the measurements in Refs. 2, 3, and 14, the present results indicate that $\bar{u}'^2/\bar{u}^2_{ref} > \bar{w}'^2/\bar{u}^2_{ref} > \bar{v}'^2/\bar{u}^2_{ref}$.

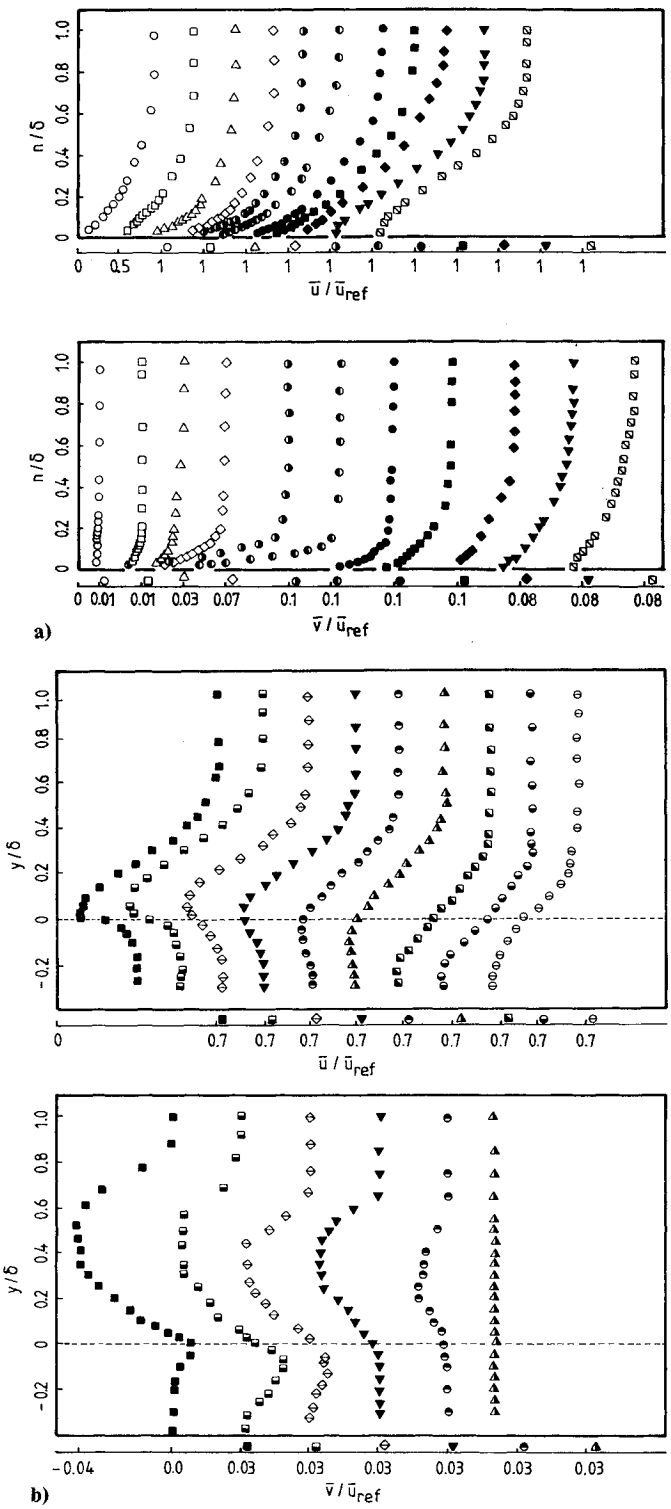

Fig. 5 Mean velocities: a) along the flap: ○, *s/c* of 0.393; □, 0.684; △, 0.706; ◇, 0.747; ○, 0.789; ○, 0.824; ●, 0.844; ■, 0.879; ◆, 0.928; ▼, 0.98; □, 0.994; and b) in the wake: ■, *x/c* of 0.00695; □, 0.0139; ◇, 0.0347; ▼, 0.0695; ○, 0.139, △, 0.209; □, 0.347; ○, 0.556; ⊖, 0.834.

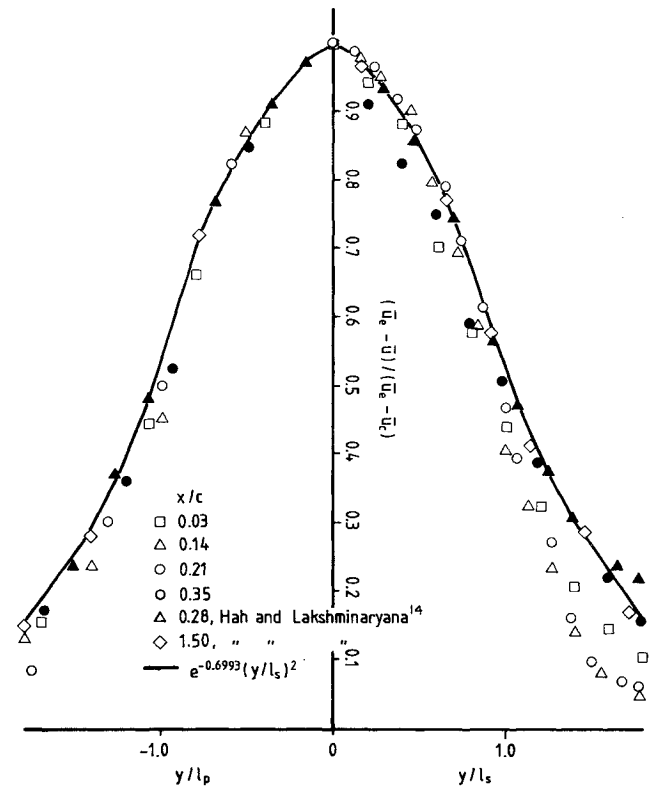

Fig. 6 Mean velocity similarity profile.

In the near wake, the largest cross-stream gradient $\partial\bar{u}/\partial y$ is at the pressure-side inflection point, but the normal intensities do not have their maximum value at this location, indicating that the turbulent kinetic energy is not linearly related to the strain rate $\partial\bar{u}/\partial y$. On the suction side, the location of minimum intensity does not coincide with the location of the minimum velocity, indicating a departure from equilibrium.

The turbulent shear stress (Fig. 8) changes sign in the neighborhood of the location of zero $\partial\bar{u}/\partial y$ (shown by an arrow in the figure) and again implies nonequilibrium behavior. The shear stress on the suction side increases due to the combined influence of adverse pressure gradient and destabilizing streamline curvature. Since shear stress is more sensitive to streamline curvature than are normal stresses, the increase is correspondingly larger, with the peak suction-side value increasing by nearly 70% between $0.0069 \leq x/c \leq 0.069$. Unlike normal stresses, the magnitude of the peak negative shear stress on the pressure side increases by a factor of 3 between $0.0069 \geq x/c < 0.069$ and then decreases until the shear stress in the pressure side is entirely positive (at $x/c = 0.347$). At 16 and 17.5 deg incidence, the shear-stress distribution and its streamwise development are more complex due to the influence of the trailing edge separation bubble. Unlike the streamwise normal stresses whose magnitudes at 14 and 16 deg deflection are of the same order, the peak suction and pressure-side shear stress at 16 deg deflection is more than twice the corresponding value at a 14 deg deflection angle.

The mixing-length distributions at three locations are shown in Fig. 9. Along the surface, the maximum L/δ values are smaller than the 0.09 value expected in zero pressure gradient flows, and unlike the results of Refs. 12 and 15, there does not appear to be a level value in the middle portion of the layer.

The local similarity of the shear-shear profile was confirmed by plotting the values of $-\overline{u'v'}/(-\overline{u'v'})_{max}$ against y/b (not shown). The results also agree well with those of Refs. 6 and 8 and with the asymptotic shear-stress profile.

Momentum and Turbulence Energy Balances

Terms in the momentum balance equation representing advection, pressure gradient, normal and shearing stress gradients and terms in the kinetic energy balance equation representing advection, production, and imbalance were calculated from the measured data in order to quantify their relative importance. The curvature terms were assumed to be small. A computer program that fits a monotone Hermite cubic spline[21] to the measured data was used.

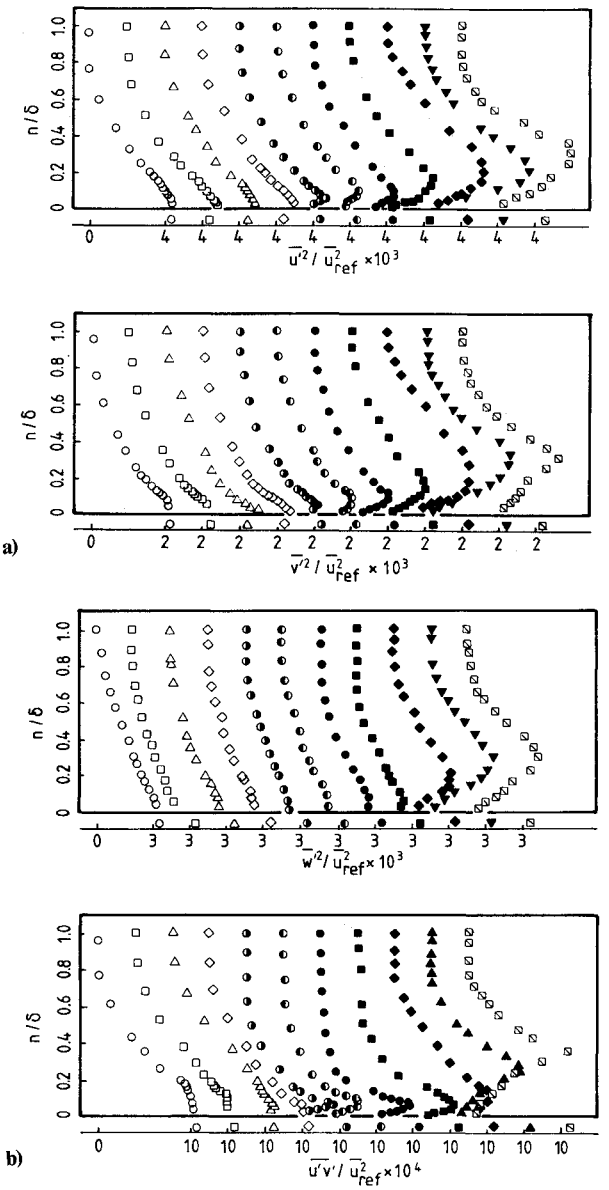

Fig. 7 Reynolds stress distributions along the suction-side surface (legend in Fig. 5).

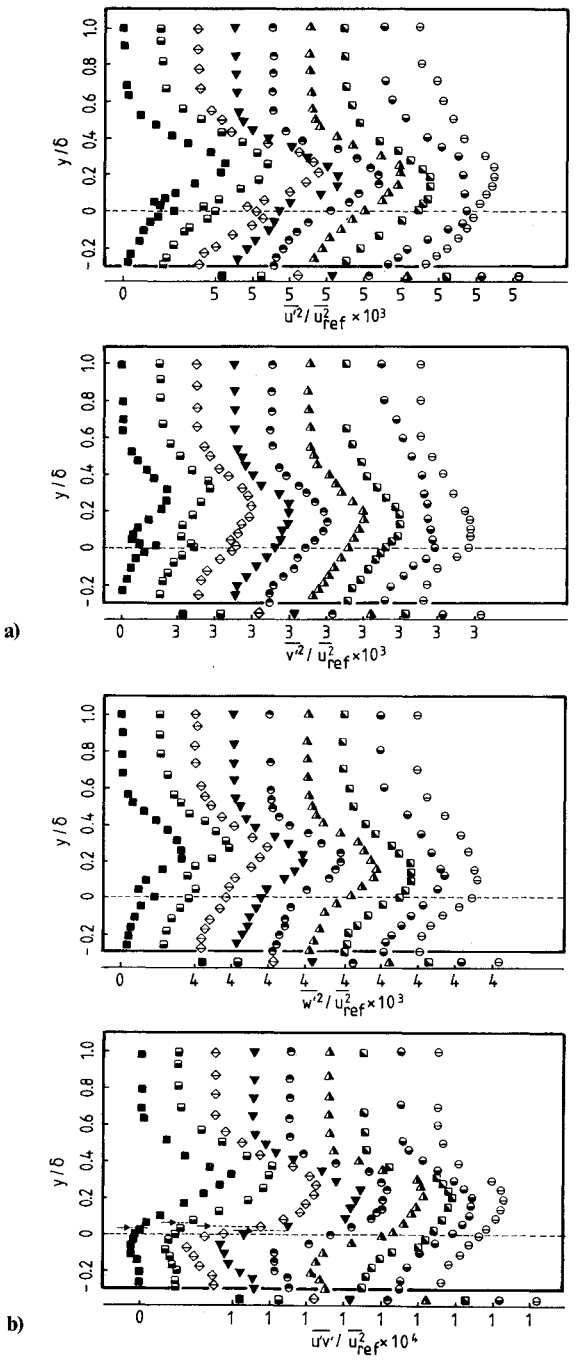

Fig. 8 Reynolds stress distributions in the wake (legend in Fig. 5).

Figure 10 shows the distribution of the terms in the streamwise momentum equation, the normal momentum equation, and the kinetic energy equation at two locations in the boundary layer ($s/c=0.817$ and 0.98) and at one location in the near wake ($x/c=0.035$). In the boundary layer, the stress gradient $\partial\bar{u}'^2/\partial x$ in the streamwise momentum equation is small compared to the dominant pressure gradient and inertial terms. Close to the wall, the shear-stress gradient $\partial\overline{u'v'}/\partial y$ is important but decays to a small value beyond n/δ of 0.5. Therefore, for $n/\delta>0.5$, the pressure gradient and inertial terms balance each other (i.e., $\bar{u}\cdot\nabla\bar{u}=-\nabla\bar{p}$). The streamwise pressure gradient $\partial\bar{p}/\partial x$ varies across the boundary layer indicating, as confirmed by the terms in the normal momentum equation, that $\partial\bar{p}/\partial y$ is nonzero. In the wake, the stress gradient $\partial\overline{u'v'}/\partial y$ is also important, and therefore this term should always be included in the momentum equation to correctly represent the details of the flow. The stress gradient terms become increasingly important with increasing angle of incidence.[2,3] The terms in the normal momentum equation are at least as important as those of the streamwise momentum equation, with the normal pressure gradient term dominant and balanced primarily by the sum of the inertial term and normal stress gradient $\partial\bar{v}'^2/\partial y$. Unlike the separated flows at

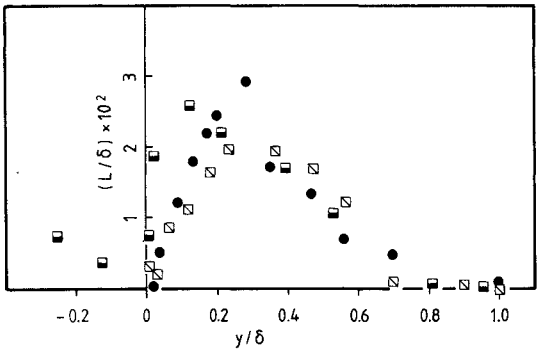

Fig. 9 Mixing-length distribution (legend in Fig. 5).

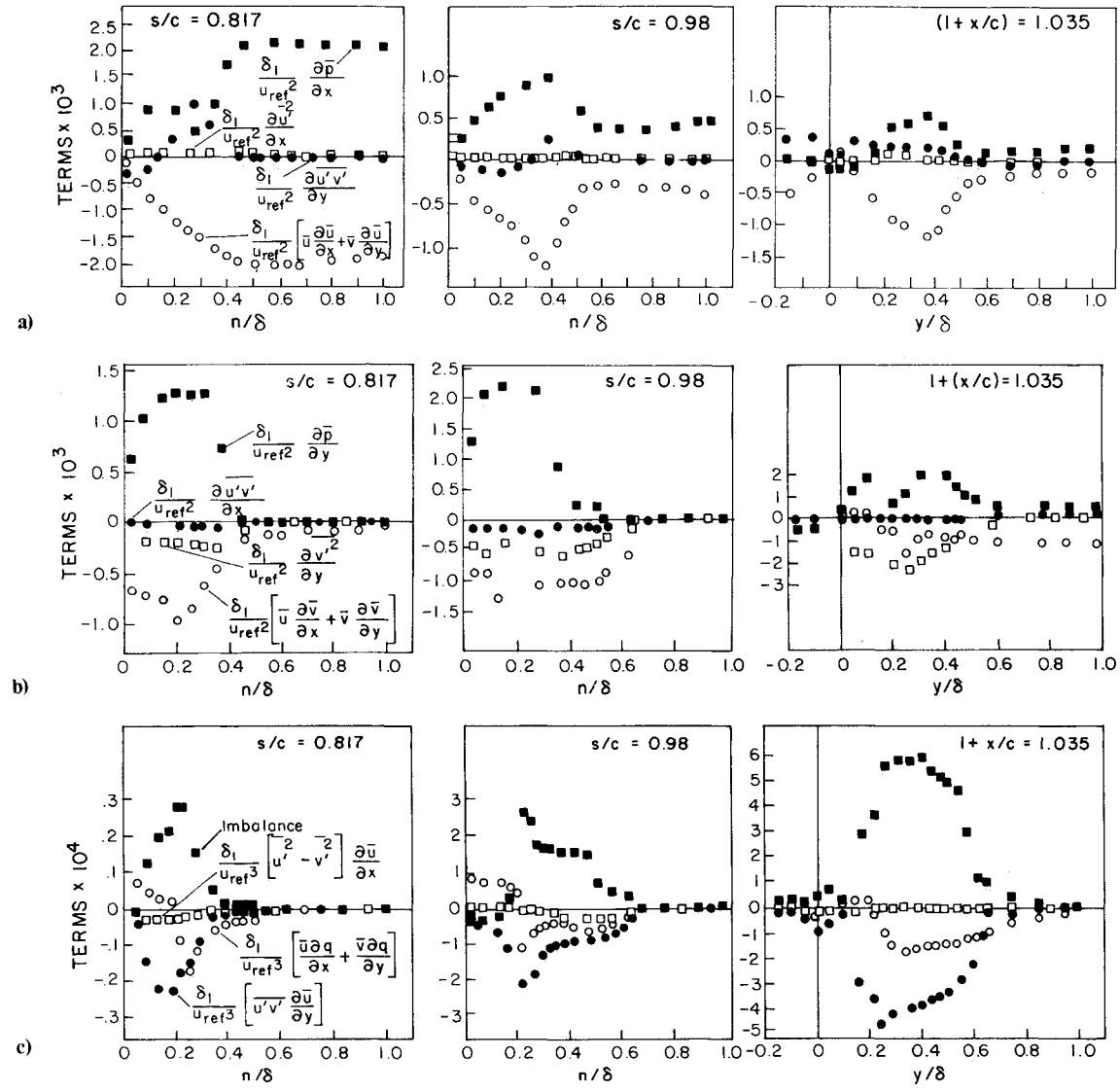

Fig. 10 Terms in the conservation equations: a) streamwise momentum equation, b) normal momentum equation, and c) kinetic energy equation.

16 and 17.5 deg incidence, the shear-stress gradient $\partial\overline{u'v'}/\partial x$ is small, and since $\partial\overline{u'^2}/\partial x$ is also small, a partially parabolized[§] form of the Navier-Stokes equation may be appropriate, except in the immediate vicinity of the trailing edge. For separated flows, the streamwise gradients of the turbulent stresses are comparable in magnitude to the cross-stream gradients, and a more complete form of the Navier-Stokes equation is required. In general, the streamwise and normal pressure gradients are of a greater magnitude than the turbulence quantities and must be represented. Only in the near-wall region and in the near wake do the turbulence quantities become as important as the pressure gradient and inertial terms.

Terms in the kinetic energy balance equation indicate that the production of energy due to normal stresses is negligible in contrast to the separated flows at 16 and 17.5 deg incidence, and again confirms the validity of the parabolized form of the Navier-Stokes equation. The dominant term in the balance equation is the shear-stress production, which peaks in the vicinity of the maximum shear stress. The imbalance term represents the sum of turbulent diffusion and viscous dissipation and also peaks near the location of maximum intensity or shear stress. As noted earlier, turbulent diffusion from the peak intensity location becomes an important mode of energy transfer to the near-wall locations, since the near-wall production of energy diminishes rapidly towards the trailing edge. In general, the production and dissipation terms do not balance each other and therefore the flow is not in local equilibrium.

Concluding Remarks

The measurements of pressure and velocity characteristics indicate that over the flap and in the near wake the flow is subjected to an adverse pressure gradient, while in the near wake immediately behind the trailing edge, there is a favorable pressure gradient. As the flow approaches the trailing edge, an inflection point is formed in the streamwise velocity profile which moves upwards with downstream distance. At the trailing edge, the flow is close to intermittent separation. The wake is observed to be asymmetric, with a destabilizing curvature on the suction side and a stabilizing curvature on the pressure side. In the near wake, the suction-side velocity profiles shows streamwise changes across the entire upper wake, but the larger variations are confined to the inner layer while in the pressure side streamwise variations are relatively small and confined to the inner layer. The destabilizing wake curvature in the suction side and the adverse pressure gradient in the

§The term "partially parabolized" implies the neglect of streamwise diffusion of viscous stresses, but not the normal pressure gradient or the normal momentum equations.

near wake cause the stresses in the near wake to increase with the shear stress increasing by as much as 60% between x/c of 0.007 and 0.035. Beyond the near wake, the mean velocity and turbulence quantities become similar, with the upper part ($y/\delta > 0$) of the wake attaining the characteristics of a symmetrical flat plate wake.

Nonequilibrium effects are noted in the near wake and imply that mixing-length models are not appropriate. Terms in the conservation equations indicate that the pressure gradient terms are of a greater magnitude than the turbulent quantities except in the near-wall region and in the very near wake. Streamwise gradients of the turbulent stresses are small and imply that a parabolized form of the Navier-Stokes equations may be adequate to describe the flow.

References

[1]Cebeci, T., Stewartson, K., and Whitelaw, J. H., "The Calculation of Two Dimensional Flow Past Airfoils," *Numerical and Physical Aspects of Aerodynamic Flows III,* Vol. 1, edited by T. Cebeci, Springer-Verlag, 1984.

[2]Thompson, B. E. and Whitelaw, J. H., "Characteristics of a Trailing Edge Flow with Turbulent Boundary Layer Separation," *Journal of Fluid Mechanics,* Vol. 157, 1985, pp. 305–326.

[3]Adair, D., "Characteristics of a Trailing Flap Flow with Small Separation," Rept. FS/84/12, Mechanical Engineering Dept., Imperial College, London, 1984 to appear in *Experiment in Fluids,* 1986.

[4]Chevray, R. and Kovasznay, L. S. G., "Turbulence Measurements in the Wake of a Thin Flat Plate," *AIAA Journal,* Vol. 7, Aug. 1969, pp. 1641–1643.

[5]Andrepoulous, J. and Bradshaw, P., "Measurements of Interacting Turbulent Shear Layers in the Near Wake of a Flat Plate," *Journal of Fluid Mechanics,* Vol. 100, 1980, pp. 639–660.

[6]Andrepoulous, J., "Symmetric and Asymmetric Near Wake of a Flat Plate," Ph. D. Thesis, Univ. of London, 1978.

[7]Ramaprian, B. R., Patel, V. C., and Sastry, M. S., "The Symmetric Turbulent Wake of a Flat Plate," *AIAA Journal,* Vol. 20, Sept. 1982, pp. 1228–1235.

[8]Pot, P. J., "Measurements in a 2-D Wake and in a 2-D Wake Merging into a Boundary Layer," Data Rept. NLR-TR-79063 U, NLR, the Netherlands, 1979.

[9]Badri Narayanan, M. A., Raghu, S., and Tulapurkara, E. G., "The Non-equilibrium Region of a Mixing Layer," *AIAA Journal,* Vol. 23, July 1985, pp. 987–991.

[10]Hoad, D. R., Meyers, J. F., Young, H. W., and Hepner, T. E., "Laser Velocimeter Survey about a NACA 0012 Wing at Low Angles of Attack," NASA TM-74040, 1978.

[11]Yu, J. C., "Mean Flow and Turbulence Measurements in the Vicinity of the Trailing Edge of a NACA 63-012 Airfoil," NASA TP 1845, 1981.

[12]Johnson, D. A. and Bachalo, W. D., "Transonic Flow Past a Symmetrical Airfoil—Inviscid and Turbulent Flow Properties," Jan. *AIAA Journal,* Vol. 18, Jan. 1980, pp. 16–24.

[13]Johnson, D. A. and Spaid, F. W., "Measurement of the Boundary Layer and Near Wake of a Supercritical Airfoil at Cruise Conditions," AIAA Paper 81-1242, 1982.

[14]Hah, C. and Lakshminarayana, B., "Measurement and Prediction of Mean Velocity and Turbulence Structure in the Near Wake of an Airfoil," *Journal of Fluid Mechanics,* Vol. 115, 1982, pp. 251–282.

[15]Nakayama, A., "Measurements of the Boundary Layer and Wake of Two Airfoil Models," Rept., MDC J2403, Aerodynamics Research Dept., Douglas Aircraft Co., Long Beach, CA, June 1982; (also *Numerical and Physical Aspects of Aerodynamics Flows,* Springer-Verlag, 1983, pp. 1–12).

[16]Viswanath, P. R., Cleary, J. W., Seegmiller, H. L., and Horstman, C. C., "Trailing Edge Flows at High Reynolds Number," *AIAA Journal,* Vol. 18, Sept. 1980, pp. 1059–1065.

[17]Crabb, D., "Jets in Crossflow," Ph.D. Thesis, Univ. of London, 1979.

[18]Bryer, D. W. and Pankhurst, R. C.,"Pressure Probe Methods for Determining Wind Speed and Flow Direction," Her Majesty's Stationery Office, London, 1971.

[19]Thompson, B. E., "The Turbulent Separating Boundary Layer and Downstream Wake," Ph.D Thesis, Imperial College, Univ. of London, 1984.

[20]Sandborn, V. A. and Kline, S. J., "Flow Models in Boundary Layer Stall Inception," *ASME Journal of Basic Engineering,* Vol. 83, 1961, pp. 317–328.

[21]Fritsch, F. N. and Carlson, R. E., "Monotone Piecewise Cubic Interpolation," *SIAM Journal of Numerical Analysis,* Vol. 17, 1980, pp. 258–244.